

Effect of ball milling and dynamic compaction on magnetic properties of Al₂O₃/Co(P) composite particles

E. A. Denisova, L. A. Kuzovnikova, R. S. Iskhakov, A. A. Bukaemskiy, E. V. Eremin, and I. V. Nemtsev

Citation: *Journal of Applied Physics* **115**, 17B530 (2014); doi: 10.1063/1.4869158

View online: <http://dx.doi.org/10.1063/1.4869158>

View Table of Contents: <http://scitation.aip.org/content/aip/journal/jap/115/17?ver=pdfcov>

Published by the AIP Publishing

Articles you may be interested in

[Influence of ball milling and annealing conditions on the properties of L10 FePt nanoparticles fabricated by a new green chemical synthesis method](#)

J. Appl. Phys. **115**, 17A732 (2014); 10.1063/1.4866553

[Microstructure and magnetic properties of C/Co-P and Al₂O₃/Co-P composite particles prepared by electroless plating](#)

J. Appl. Phys. **113**, 17A340 (2013); 10.1063/1.4800037

[Crystallographic alignment evolution and magnetic properties of Nd-Fe-B nanoflakes prepared by surfactant-assisted ball milling](#)


J. Appl. Phys. **111**, 07A732 (2012); 10.1063/1.3679414

[Anisotropic SmCo₅ flakes and nanocrystalline particles by high energy ball milling](#)

J. Appl. Phys. **109**, 07A728 (2011); 10.1063/1.3562447

[Magnetic anisotropy and crystal structure of Co-P films synthesized by electrodeposition from alkaline electrolytes](#)

J. Appl. Phys. **99**, 08M304 (2006); 10.1063/1.2167328

The advertisement is set against a dark blue background with a subtle wave pattern. It is divided into three main sections. The left section features a photograph of a silver and black AFM headstage. The middle section shows a grey tombstone with the inscription 'RIP My Old AFM 1994-2015'. The right section features a man in a white shirt and tie, looking distressed with his hands raised. Text is overlaid on these images. On the right side, there is a large white text block with orange and white text, and the Oxford Instruments logo at the bottom right.

Frustrated by old technology?

Is your AFM dead and can't be repaired?

Sick of bad customer support?

It is time to upgrade your AFM

Minimum \$20,000 trade-in discount for purchases before August 31st

Asylum Research is today's technology leader in AFM

dropmyoldAFM@oxinst.com

OXFORD
INSTRUMENTS
The Business of Science®

Effect of ball milling and dynamic compaction on magnetic properties of $\text{Al}_2\text{O}_3/\text{Co(P)}$ composite particles

E. A. Denisova,^{1,2} L. A. Kuzovnikova,² R. S. Iskhakov,^{1,a)} A. A. Bukaemskiy,³ E. V. Eremin,¹ and I. V. Nemtsev⁴

¹Kirensky Institute of Physics SB RAS, Krasnoyarsk, Russian Federation

²Krasnoyarsk Institute of Railways Transport, Krasnoyarsk, Russian Federation

³Institut für Sicherheitsforschung und Reaktortechnik, D-52425 Juelich, Germany

⁴Krasnoyarsk Scientific Center SB RAS, Krasnoyarsk, Russian Federation

(Presented 7 November 2013; received 21 September 2013; accepted 17 January 2014; published online 20 March 2014)

The evolution of the magnetic properties of composite $\text{Al}_2\text{O}_3/\text{Co(P)}$ particles during ball milling and dynamic compaction is investigated. To prepare starting composite particles, the Al_2O_3 granules were coated with a Co_9P_5 shell by electroless plating. The magnetic and structural properties of the composite particles are characterized by scanning electron microscopy, X-ray diffraction, and the use of the Physical Property Measurement System. The use of composite core-shell particles as starting powder for mechanoactivation allows to decrease treatment duration to 1 h and to produce a more homogeneous bulk sample than in the case of the mixture of Co and Al_2O_3 powders. The magnetic properties of the milled composite particles are correlated with changes in the microstructure. Reduction in grain size of Co during milling leads to an increase of the volume fraction of superparamagnetic particles and to a decrease of the saturation magnetization. The local magnetic anisotropy field depends on the amount of hcp-Co phase in sample. The anisotropy field value decreases from 8.4 kOe to 3.8 kOe with an increase in milling duration up to 75 min. The regimes of dynamic compaction were selected so that the magnetic characteristics—saturation magnetization and coercive field—remained unchanged. © 2014 AIP Publishing LLC.

[<http://dx.doi.org/10.1063/1.4869158>]

I. INTRODUCTION

Ceramometals (cermets), consisting of uniformly dispersed ferromagnetic metallic particles into an oxide matrix, have been the subject of intensive study due to their unique combination of magnetic and mechanical properties: enhanced microwave absorption,¹ giant magnetoresistance,² and good catalytic properties³ without losing of mechanical properties of monolithic Al_2O_3 ceramic. Usually cermets are manufactured from a mixture of metallic and oxide powders, that is, pressed and sintered at high temperatures;⁴ several chemical methods are used as well.^{5,6} However, retaining nanometric grain sizes during powder consolidation techniques is difficult. Thus, producing bulk nanostructured materials still remains relevant. Another way to prepare cermets is based on the mechanical alloying of various metals with aluminum or Al_2O_3 powder.^{7,8} The ball milling has been demonstrated to be able to perform mechanochemical synthesis (MS), to grind powders to nanometric scale, and to produce large quantities of material for a low cost. It was found^{9,10} that the desired mechanical properties (fracture toughness) of bulk cermets can be achieved by introducing Co particles with certain hcp/fcc phase ratio. However, to prepare cermet by traditional MS, long treating time is needed, reaching up to 16–20 h of treating in a high energy ball mill. In previous research,¹¹ we show that the use of composite core-shell particles as starting powder for MS decreases treatment duration

to 1–2 h. In this paper, we utilize the same approach to produce the $\text{Al}_2\text{O}_3/\text{Co(P)}$ cermet (i.e., we use the core-shell particles as starting powder for MS in order to reduce the time needed to prepare the composite particles with optimal hcp/fcc phase ratio).

In the present work, we report on the evolution of structural and magnetic properties of $\text{Al}_2\text{O}_3/\text{Co(P)}$ composite particles during ball milling and dynamic compaction processes. We show that the magnetic properties of the composites depend strongly on the microstructure created during the mechanical activation in the planetary ball mill, and that the use of composite core-shell particles allows us to produce a more homogeneous bulk sample than in the case of the mixture of Co and Al_2O_3 powders.

II. EXPERIMENTAL

The initial $\text{Al}_2\text{O}_3/\text{Co(P)}$ composite particles consist of granular Al_2O_3 cores (50 mass %), surrounded by a shell of Co_9P_5 particles. The Co-P particles was deposited on Al_2O_3 surface by electroless plating as described in our previous study.¹² The milling of the composite particles was performed in planetary ball mill AGO-2U with stainless-steel vials and balls during 15, 30, 45, 60, 75, and 90 min. The ball-to-powder weight ratio is 20:1. The Co_9P_5 particles were also milled under the same conditions. The morphology and the composition of the powders were analyzed using scanning electron microscopes (SEM) (Carl Zeiss EVO 60 and Hitachi TM3000 with Xflash 430 H detector, Bruker)

^{a)}Electronic mail: rauf@iph.krasn.ru.

and an energy-dispersive spectrometer (EDS) (INCA, Oxford Instruments). The crystalline structure of the composite powders was determined using a DRON-4 X-ray diffractometer operating with Cu K α radiation. The field and low-temperature dependences of magnetization, $M(T,H)$, were measured in the external field range up to 50 kOe and at 4.2–300 K using a Physical Property Measurement System (PPMS). The bulk composite samples were prepared by dynamic compaction.¹³

III. RESULTS AND DISCUSSION

The SEM images of the initial composite particles are presented at Fig. 1(a). It can be seen that the shape of the Co(P) particles is nearly spherical for Al₂O₃/Co₉₅P₅ composite powders. The average Co₉₅P₅ particle size supported on the surface of Al₂O₃ granules is 200 nm. Figures 1(b) and 1(c) show SEM images of the Al₂O₃/Co(P) composite particles ball milled during 45 and 75 min, respectively. After milling the particles were plastically deformed, and flattened particles were broken to smaller pieces. The majority of the particles contained both Al₂O₃ and Co(P), as revealed by EDS analysis (Fig. 2). After 45 min of milling, the average particle size increases, while we observe a wider particle size distribution. It should be noted that ductility of Al₂O₃/Co(P) composite increases after treating for 45 min. When milling time reaches 75 min the volume fraction of particles with size smaller than 100 nm increases.

The XRD patterns of the Al₂O₃/Co₉₅P₅ powders after ball milling for various treatment durations are shown in Fig. 2(d). The initial Al₂O₃/Co₉₅P powder XRD pattern corresponds to the hcp Co phase and Al₂O₃. For the sample with 15 min milling time, XRD peaks corresponding to the Co hcp phase and those corresponding to the Co fcc phase are presented together. As the milling time reaches 45 min, the XRD analysis indicates the presence of Co fcc phase, while the Co hcp peaks further weaken. Such transformations of Co hcp phase to Co fcc phase during milling have been frequently observed.^{14,15} The XRD analysis reveals that the pure Co₉₅P₅ powder milling causes following transformations: hcp Co(P) \rightarrow fcc Co(P) \rightarrow amorphous state \rightarrow hcp Co(P) after 30, 60, and 90 min of milling duration, respectively. Evidently, the hard Al₂O₃ particles prevent the amorphous state formation during ball milling of composite particles.

The hysteresis loops of the initial Al₂O₃/Co(P) composite powders and milled powders are shown in Fig. 3. The coercivity values insignificantly grow after ball milling

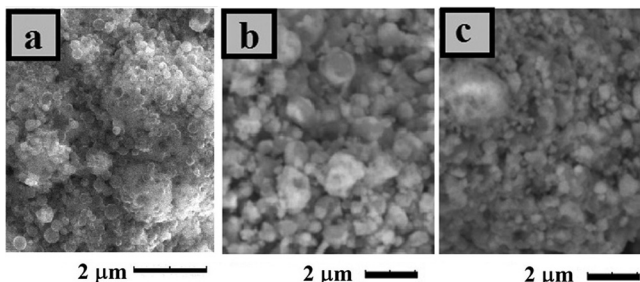


FIG. 1. Scanning electron micrograph of the Al₂O₃/Co₉₅P₅ composite particles before (a), and after ball milling: (b) during 45 min, (c) 75 min.

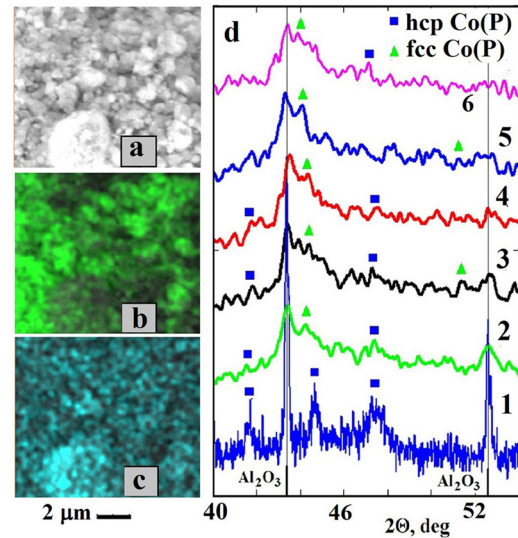


FIG. 2. SEM image of Al₂O₃/Co₉₅P₅ particles milled for 45 min. (a) The images in (b) and (c) are the corresponding Co and Al EDX mappings of the composite particles milled for 45 min; (d) XRD spectra of the Al₂O₃/Co₉₅P₅ composite powders for (1) initial and (2) 15 min, (3) 30 min, (4) 45 min, (5) 60 min, and (6) 75 min of milling time.

($H_c \sim 300$ Oe for 75 min milled powder). The inset on Fig. 3 shows the temperature dependence of magnetization for the Al₂O₃/Co(P) composites before and after treating in the planetary ball mill. We fit the $M(T)$ curve with the following equation:

$$M(T) = A(1 - BT^{3/2}) + CL\left(\frac{D}{T}\right), \quad (1)$$

where $M(T)$ is magnetization of Al₂O₃/Co(P) particles at temperature T , B is the Bloch constant, $L(x)$ is the Langevin function, $A = M_f V_f$, $C = M_{sp} V_{sp}$, and D are fitting constants. Here, M_f is the average magnetization of the ferromagnetic phase, V_f is the volume fraction of this phase, M_{sp} is the average magnetization of the superparamagnetic phase, V_{sp} is the volume fraction of this phase. The first term corresponds to

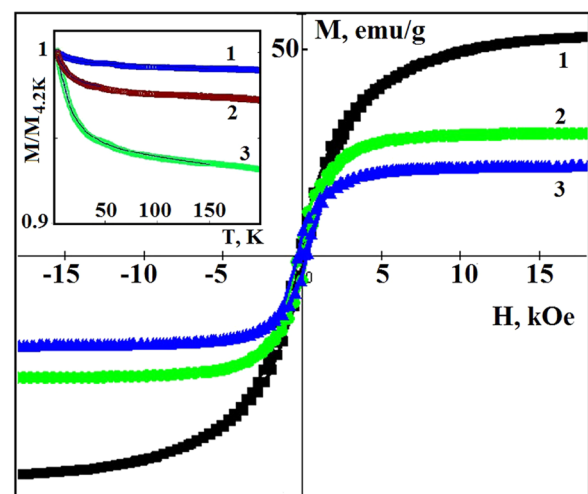


FIG. 3. The hysteresis loops measured at room temperature for Al₂O₃/Co₉₅P₅ composite particles (1-black rhomb), and ball milled for 15 min (2-green circle), for 75 min (3-blue triangle). Inset show the temperature dependence of magnetization for the Al₂O₃/Co₉₅P₅ (1) composites and powders ball milled during 15 min (2) and 75 min (3).

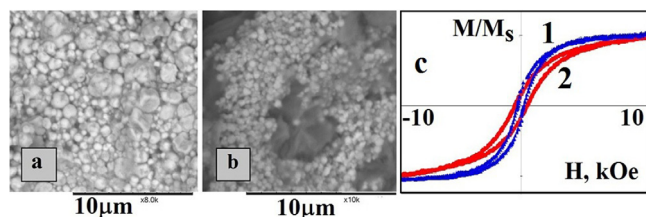


FIG. 4. SEM images of the bulk materials produced by dynamic compaction of the $\text{Al}_2\text{O}_3/\text{Co}_{95}\text{P}_5$ composite particles (a) and mixture of Al_2O_3 and Co_{95}P_5 (b) powders. The shiny areas in (a) and (b) correspond to Co, whereas the darker ones to Al_2O_3 . (d) The hysteresis loops of the bulk materials prepared from the composite particles (1) and the mixture of powders (2).

the contribution of the ferromagnetic phase. The second term represents the contribution of the superparamagnetic ultra-thin ferromagnetic clusters not coupled by exchange. The fitting results indicate that the V_{sp} significantly increases with milling duration. The $V_{sp} \sim 2\%$ for initial particles and $V_{sp} \sim 12\%$ for $\text{Al}_2\text{O}_3/\text{Co(P)}$ particles milled during 75 min. This is consistent with the decrease of magnetization value of $\text{Al}_2\text{O}_3/\text{Co(P)}$ powders during the milling process. The magnetization is 54 emu/g for initial $\text{Al}_2\text{O}_3/\text{Co(P)}$ particles and it is equal to 22 emu/g for $\text{Al}_2\text{O}_3/\text{Co(P)}$ particles milled during 75 min. Such a decrease of magnetization value has not been observed for $\text{Co}/20\text{mass}\%-\text{Al}_2\text{O}_3$ and $\text{Co}/50\text{mass}\%-\text{Al}_2\text{O}_3$ for milling duration up to 20 h.⁸ The decrease of magnetization value was observed for $\text{Al}_2\text{O}_3/42\text{ mass}\%-\text{Co(P)}$ powders during the milling process.⁷ It is likely that the magnetization decreases depends on the milling energy (i.e., mechanically driven transformation).

Information on the local anisotropy field and the grain size in the systems of exchange-coupled grains can be obtained from investigation of approach magnetization to saturation law.^{16–18} Approach to magnetic saturation curves in the applied fields up to $7 \div 50$ kOe for the all nanocomposites follow Akulov's law: $M(H) = M_0(1 - aH_a^2/H^2)$, where $H_a = 2K/M_s$ is the local magnetic anisotropy field and a is the symmetry coefficient. This allows us to calculate the local magnetic anisotropy field H_a . Despite the increase in microstrain, the H_a value decreases from 8.4 kOe to 3.8 kOe with an increase in milling duration up to 75 min. Such H_a behavior reflects the transformation of highly anisotropic Co hcp phase to Co fcc phase during the milling process.

Figure 4 shows SEM images of bulk cermet produced by dynamic compaction of the composite $\text{Al}_2\text{O}_3/\text{Co}_{95}\text{P}_5$ powder (a)—sample I and mixture of Al_2O_3 and Co_{95}P_5 powders (b)—sample II. It can be noticed that the sample II is characterized by larger inhomogeneous microstructure. Such layered microstructure of sample II causes an increase of the coercivity values up to 400 Oe. The coercivity H_c of sample I is 200 Oe (Fig. 4(c)), i.e., the H_c value basically stays constant during the compacting process. It is found that the local

magnetic anisotropy field H_a remains unchanged after the compaction process for sample II. In the case of composite particles compaction the grain size increases and it leads to a decrease of H_a value to 3 kOe.

IV. CONCLUSIONS

In summary, the structural and magnetic properties of $\text{Al}_2\text{O}_3/\text{Co}_{95}\text{P}_5$ composite powders have been investigated. The ball milled composite powders consist of a mixture of hcp and fcc phases. It is found that the volume fraction of superparamagnetic particles significantly increases in the course of the milling process up to 12 vol. %. Reduction in grain size of Co leads to a decrease of the saturation magnetization. In spite of having somewhat lower value of magnetization, composite particles passed through the 45 min ball milling process possess a high enough value of ductility necessary to produce a bulk material with the best combination of magnetic and mechanical properties. In other words, we sacrifice magnetization value for better mechanical properties such as improvement in bending strength and fracture toughness. Also, the ball milling causes the H_a value to significantly decrease. Such H_a behavior reflects the transformation of the highly anisotropic Co hcp phase to the Co fcc phase during the milling process. Magnetic measurements show that the coercivity remains unchanged after dynamic compaction. Using the composite particles as starting powder for the compacting process allows us to produce a more homogeneous bulk sample than in the case of the mixture of Co and Al_2O_3 powders.

ACKNOWLEDGMENTS

This work was partially supported by Russian Foundation of Basic Research 13-03-00476-a.

- ¹T. Fujieda *et al.*, J. Jpn. Inst. Met. **66**(3), 135 (2002).
- ²J. Q. Xiao *et al.*, Phys. Rev. Lett. **68**, 3749 (1992).
- ³A. S. Andreev *et al.*, Adv. Mater. Res. **702**, 79 (2013).
- ⁴X. DeVaux and A. Rousset, U.S. patent 5,462,903 (31 October 1995).
- ⁵T. Lu and Y. Pan, J. Mater. Sci. **45**, 5923 (2010).
- ⁶S.-T. Oh *et al.*, J. Mater. Sci. Lett. **21**, 275 (2002).
- ⁷J. Li *et al.*, J. Alloys Compd. **440**, 349 (2007).
- ⁸E. Menéndez *et al.*, J. Mater. Res. **22**, 2998 (2007).
- ⁹S. I. Cha *et al.*, Int. J. Refract. Met. Hard Mater. **19**, 397 (2001).
- ¹⁰W. Tai and T. Watanabe, J. Mater. Sci. **33**, 5795 (1998).
- ¹¹R. S. Iskhakov *et al.*, J. Optoelectron. Adv. Mater. **10**, 1043 (2008).
- ¹²E. A. Denisova *et al.*, J. Appl. Phys. **113**, 17A340 (2013).
- ¹³V. A. Ignatchenko *et al.*, Sov. Phys. JETP **55**, 878 (1982).
- ¹⁴L. Kuzovnikova *et al.*, Solid State Phenom. **190**, 192 (2012).
- ¹⁵J. X. Huang *et al.*, Nanostruct. Mater. **4**, 293 (1994).
- ¹⁶V. K. Portnoi *et al.*, Neorg. Mater. **40**, 937 (2004).
- ¹⁷E. M. Chudnovsky *et al.*, Phys. Rev. B **33**, 251 (1986).
- ¹⁸R. S. Iskhakov and S. V. Komogortsev, Phys. Met. Metallogr. **112**, 666 (2011).